Hindawi Publishing Corporation
Journal of Nanomaterials
Volume 2012, Article ID 174353, 8 pages
doi:10.1155/2012/174353

Research Article

Synthesis and Characterizations of Poly(3-hexylthiophene) and Modified Carbon Nanotube Composites

Mohammad Rezaul Karim

Center of Excellence for Research in Engineering Materials, College of Engineering, King Saud University, P.O. Box 800, Riyadh 11421, Saudi Arabia

Correspondence should be addressed to Mohammad Rezaul Karim, mkarim@ksu.edu.sa

Received 14 February 2012; Revised 12 May 2012; Accepted 14 May 2012

Academic Editor: Sevan P. Davtyan

Poly(3-hexylthiophene) and modified (functionalized and silanized) multiwall carbon nanotube (MWNT) nanocomposites have been prepared through in situ polymerization process in chloroform medium with $FeCl_3$ oxidant at room temperature. The composites are characterized through Fourier transfer infrared spectroscopy (FT-IR), Raman, and X-ray diffraction (XRD) measurements to probe the nature of interaction between the moieties. Optical properties of the composites are measured from ultraviolet-visible (UV-Vis) and photoluminescence (PL) spectroscopy. Conductivity of the composites is followed by four probe techniques to understand the conduction mechanism. The change (if any) in C=C symmetric and antisymmetric stretching frequencies in FT-IR, the shift in G band frequencies in Raman, any alterations in λ_{max} of UV-Vis, and PL spectroscopic measurements are monitored with modified MWNT loading in the polymer matrix.

1. Introduction

Conjugated polymers are being developed as alternatives to traditional inorganic semiconductors for low-cost electronic or optical devices because of the ease of their solution processing and their mechanical flexibility. Polythiophene-based composites are in the forefront. Carbon nanotubes are the most recently tried electron acceptor materials. In the case of carbon nanotubes, because of their anisotropy and presence of semiconducting tubes, the realization of its full potentiality is still a challenging task. Recently, people have attempted to bring in directionality to the orientation of the carbon nanotubes and attempts made to separate out the metallic part of carbon nanotubes exploiting the differential interaction with planar aromatic molecules, such as free-based porphyrin or pyrene with long alkyl chains [1]. Also, the transport properties of conducting polymers are known to be greatly influenced by the chemical instauration surrounding the polymer backbone, besides favorable conformation of the side chains present. Polymeric composites with multiwall carbon nanotubes can provide a good conductive path at relatively low carbon contents, as these have high aspect ratio specific surfaces and cost effective [2–5]. Hence their uses in various applications for optoelectronic devices such as organic LED, solar cells, and super capacitors and so forth. are very much anticipated.

In organic-photovoltaic devices, fullerenes [1, 2], nanoparticles [3, 4], carbon nanotubes [5–8] and conjugated polymers with high electron affinity [9–11] are being used to hybrid with semiconducting polymers like polythiophene or poly(p-phenylene vinylene) (PPV) [12]. Since the first report of a polymer/SWNT photovoltaic device in 2002, increased interest in such types of composites is evident from the very large number of publications on polythiophene (PTh)/carbon nanotube (CNT) composites that are appearing periodically with more and more innovative ideas for the creation of an effective interface between the PTh and CNT. Electron-hole pairs are generated at the interface of the polymer and CNT upon illumination. The carbon nanotubes serve as electron traps as they have more electron affinities than the conjugate polymers. MWNTs are more stable in air than fullerenes and are also much cheaper. They are also

excellent electrical conductors and they eliminate the charge transport barriers of hopping between acceptor molecules. The general methods to prepare polymer-CNT composites are (i) ultrasonication of CNT or surface functionalized CNT in presence of matrix polymers, (ii) the in situ polymerization of monomers in the presence of CNT, and (iii) polymerization of the matrix polymer from the surface of the nanotubes. In these cases, a nanohybrid/nanoconjugate is to be formed depending upon the interaction between the polymer and the CNT. In addition to intensive and intimate interfaces being formed between them, there is an additional advantage of easy solubilization in many organic solvents.

Considering all these aspects, recently direct polymerization of monomers in a CNT-dispersed medium through functionalization/nonfunctionalization of CNT has drawn great attention to prepare polymer-wrapped CNT [13–20]. The supramolecular approach of noncovalent modifications of CNT seems attractive as it will not disrupt the extended π-networks and open up the possibilities of being able to organize the nanotubes in the ordered polymer matrix. In this direction, in-situ synthesis and characterization of soluble poly(3-hexylthiophene) (P3HT) and modified (functionalized and silanized) MWNT composites have been attempted as a first report. The morphology, microstructure, and physical properties, including thermal and electrical aspects, are discussed in detail. A close look at the interface between the polymer and MWNT is made out to understand the nature of the interaction between them and their potentiality to use as photovoltaic devices junction materials.

2. Experimental Methods

General: MWNT (AP-grade, diameter: 1012 nm, and length: $2\sim20\,\mu m$) supplied by Iljin Nanotech Co., Ltd., Republic of Korea was used in as-procured form. 3-hexylthiophene (3HT) monomer (97%), chloroform, iron (III) chloride anhydrous (oxidant), 3-aminopropyltriethoxysilane, and other organic solvents purchased from Aldrich with reagent grade were used without further purification.

2.1. MWNT Functionalization. 400 mg of raw MWNT (rMWNT) was suspended in a 3 : 1 mixture of concentrated HNO_3/H_2SO_4 solution and ultrasonicated in the water bath for 24 h at 60°C using a Branson Sonifier. The resulting acid-treated MWNTs were filtered and then washed with water and methanol, subsequently. The functionalized MWNTs (fMWNT) were dried in a vacuum oven at 110°C for 24 h.

2.2. Silane-Modified fMWNT. The acid-treated MWNTs were then surface-modified using silane compounds by the following way: 200 mg of fMWNT was suspended in 100 ml of toluene and ultrasonicated in the water bath for 30 min at room temperature. 11.4 mmol of 3-aminopropyltriethoxysilane dissolved in 1 wt.% toluene solution was slowly added to the above solution and refluxed at 75°C with continuous stirring for 6 h. The solution was filtered with adding 30 ml of methanol for dilution and washed by deionized water, methanol, and acetone. The resultant silane-modified MWNT (siMWNT) powder was collected after vacuum drying at 80°C for 12 h.

2.3. Preparation of P3HT and P3HT-MWNT Nanoparticles. A typical in-situ chemical oxidative polymerization was carried out for synthesis of 3HT and 3HT-MWNT nanoparticles. The synthesis of the P3HT-MWNT nanoparticles consists of the following steps: 100 ml of $CHCl_3$ solution containing MWNT (required amounts of rMWNT, fMWNT, and siMWNT individually) was added to a 250 ml double-neck, round bottomed flask carrying a magnetic Teflon-coated stirrer. The mixture was sonicated for 1 h at room temperature in order to disperse the MWNT. 4 mmol of $FeCl_3$ in 100 ml $CHCl_3$ solution was added to the above solution and further sonicated for 30 min. 3HT monomer (1 mmol) in a 25 ml $CHCl_3$ solution was taken in a condenser and added dropwise to the MWNT and $FeCl_3$ solution with constant stirring. The reaction mixture was stirred for an additional 24 h under the same conditions. The resultant MWNT-P3HT composite was precipitated in methanol, filtered using a Buchner funnel, and then carefully washed several times with methanol, 0.1 M HCl, deionized water and acetone. The obtained black powder was dried under a vacuum dryer at room temperature for 24 hrs. The 3HT polymerization (P3HT) was done following a similar procedure by using the same monomer and oxidant ratios with the absence of carbon nanotubes.

2.4. Characterizations. X-ray diffractions were measured using a XRD-7000 (Shimadzu, Japan). The X-ray beam was Cu Kα (λ = 0.1541 nm) radiation from a sealed tube operated at a 40 kV voltage and a 25 mA current and was calibrated with a standard silicon sample. The samples were scanned from $2\theta = 0°$ to 60° at the step scan mode (step size 0.02°) at a scan rate of 1.2°/min, and the diffraction pattern was recorded using a proportional detector. Fourier transform infrared (FT-IR) spectra of the samples were performed from a KBr pellet of the nanocomposites in a Thermo 5700 model instrument. Raman spectra of the solid samples were taken at the excitation wavelength of 780 nm using a Thermo Almega XR model. Ultraviolet-visible spectra (UV-Vis) of the P3HT and the P3HT-MWNT composites were recorded using a UV-3600 UV/Vis/NIR spectrometer (Shimadzu, Japan) in a 1, 2, 4-trichlorobenzene solvent at room temperature from 200 to 800 nm. Photoluminescence experiments of the polymer and the nanocomposite solutions were performed with a RF-5301PC spectrometer (Shimadzu, Japan). For the FE-SEM study, a dried film of the polymer and composites was platinum coated and was observed through a field emission scanning electron microscope (JSM-7800F; JEOL, Japan) at 20 kV. The dispersity of carbon nanotubes in the polymer matrix was studied using a JEM-2100F (JEOL, Japan) operated at an accelerated voltage of 100 kV. A drop of diluted solution of the polymer/composite in ethanol dispersed by sonication on the carbon-coated copper grid was dried finally in a vacuum and was directly observed in the TEM. Thermal stability of the polymer/composite was measured using a

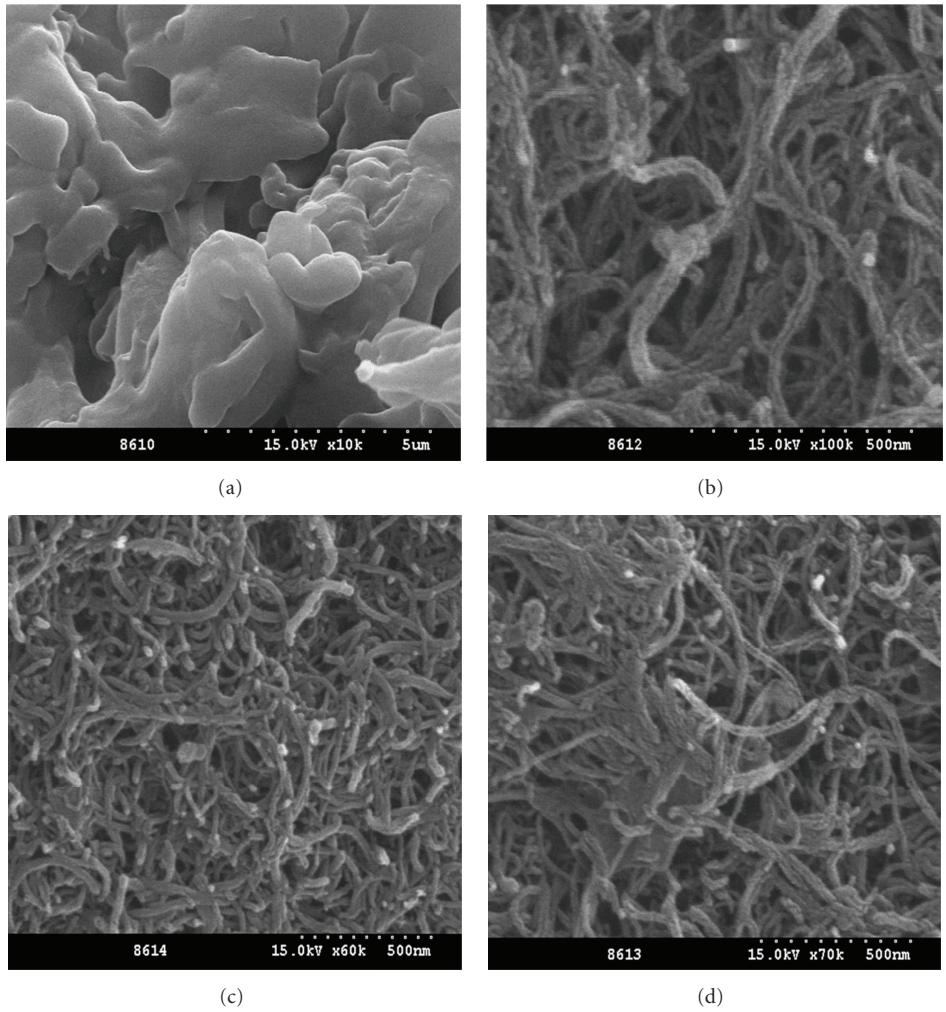

(a) (b)

(c) (d)

Figure 1: FE-SEM images of (a) P3HT and P3HT-MWNT composites of (b) P3HT-rMWNT, (c) P3HT-fMWNT, and (d) P3HT-siMWNT.

Seiko, TG/DTA 320 under a nitrogen atmosphere at a heating rate 10°C/min. The room temperature conductivity of the pressed pellets was measured with the standard four-point probe method, using a Jandel engineering instrument, model CMTSR1060N.

3. Results and Discussion

Typical FE-SEM images of the P3HT and P3HT/MWNT nanocomposites are presented in Figure 1. By comparing them one can see the well-buried MWNT in the polymer matrix taking tubular structures. The TEM picture presented in Figure 2 presents a closer view of MWNT with polymer wrappings.

The electron-diffractive X-ray (EDX) analysis data of the polymer and the composites (Figure 3) show that there is a slight increase in the carbon content of the composite with a substantial decrease in the weights of sulfur and hydrogen, indicating the formation of the composites. Figure 3(c) presents silane group attachment successfully.

The X-ray diffraction patterns obtained at room temperature are presented in Figure 4. The scattering peaks at 5.18 and 23.8°2θ arise from the first and higher order reflections from large length d-spacing for P3HT [21–23] and correspond to the in-plane interchain distance. The amorphous halo wide-angle peak with lesser intensity appears at 23.8°2θ, which represents the stacking distance of the thiophene rings or interplanar distance. There is little shifting in the scattering peaks' positions with the addition of MWNT with respect to interplane and intrachain distances. And, the full-width at half-maximum (FWHM) suggests some changes in the crystallite size values. This could be due to the physical wrapping of the polymer on the walls of the nanotubes. The layered structure, with maximum chains forming parallel planes and side chains acting as spacers, is typical for a comb-like polymer in general indexed as (h00) (h.1,2,3, ...) and the corresponding d-spacing values can well imply the spacing between adjacent back bone chains [24–28].

The FT-IR spectra of the P3HT and P3HT-MWNT composites are shown in Figure 5. Theoretical investigation reveals that monocrystalling graphite belongs to the D^4_{6h}

(a) (b) (c)

Figure 2: TEM images of (a) P3HT-rMWNT, (b) P3HT-fMWNT, and (c) P3HT-siMWNT composites.

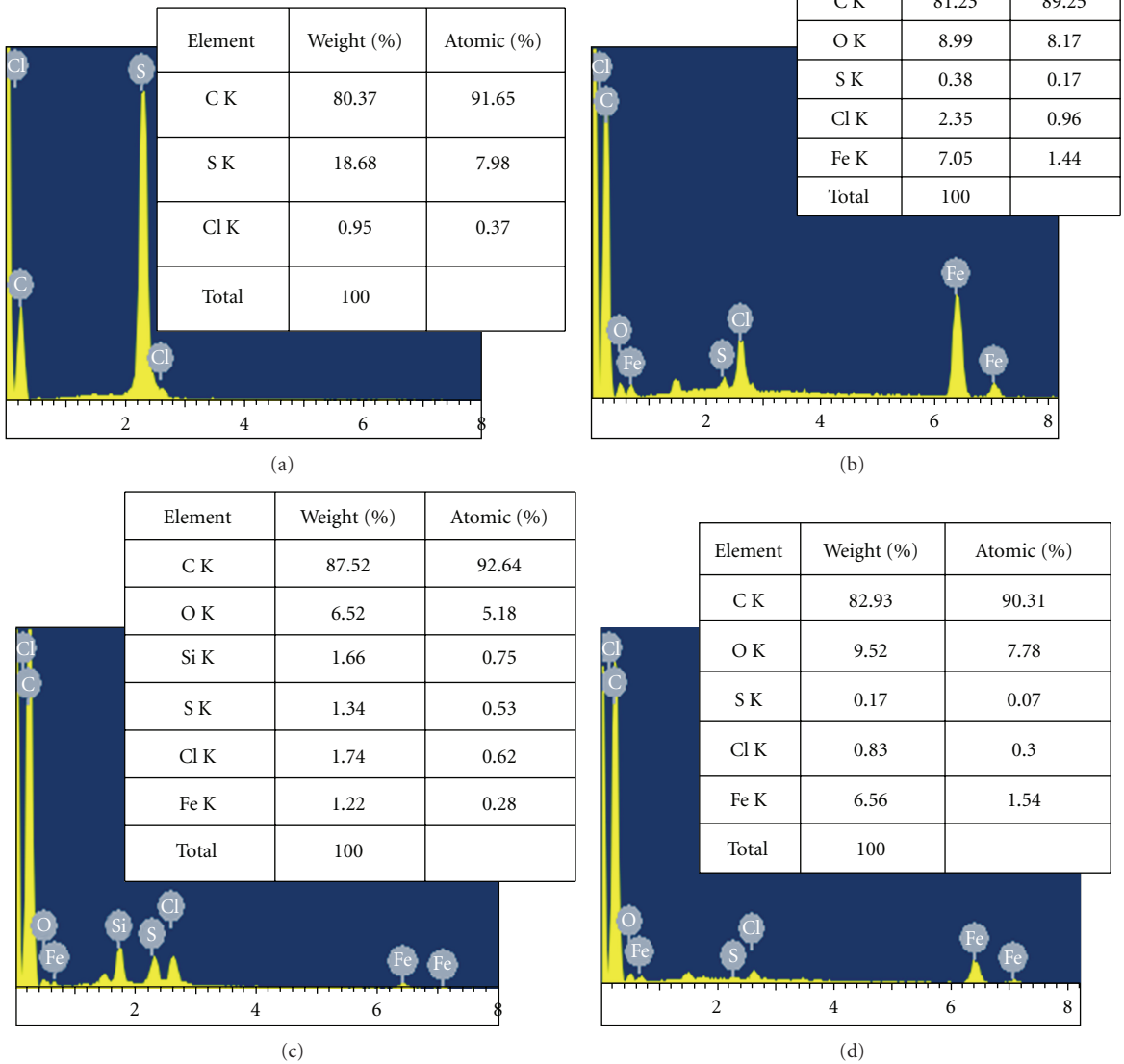

(a)

Element	Weight (%)	Atomic (%)
C K	80.37	91.65
S K	18.68	7.98
Cl K	0.95	0.37
Total	100	

(b)

Element	Weight (%)	Atomic (%)
C K	81.23	89.25
O K	8.99	8.17
S K	0.38	0.17
Cl K	2.35	0.96
Fe K	7.05	1.44
Total	100	

(c)

Element	Weight (%)	Atomic (%)
C K	87.52	92.64
O K	6.52	5.18
Si K	1.66	0.75
S K	1.34	0.53
Cl K	1.74	0.62
Fe K	1.22	0.28
Total	100	

(d)

Element	Weight (%)	Atomic (%)
C K	82.93	90.31
O K	9.52	7.78
S K	0.17	0.07
Cl K	0.83	0.3
Fe K	6.56	1.54
Total	100	

Figure 3: EDX data of (a) bulk P3HT and P3HT-MWNT composites of (b) P3HT-rMWNT, (c) P3HT-siMWNT, and (d) P3HT-fMWNT.

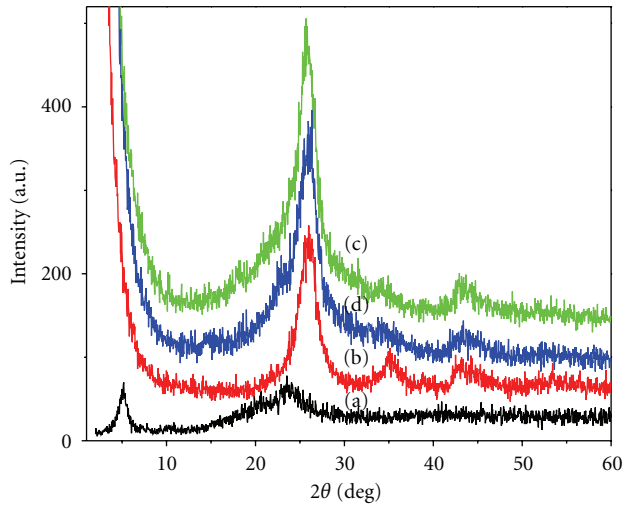

FIGURE 4: XRD data of (a) bulk P3HT and P3HT-MWNT composites of (b) P3HT-rMWNT, (c) P3HT-siMWNT, and (d) P3HT-fMWNT.

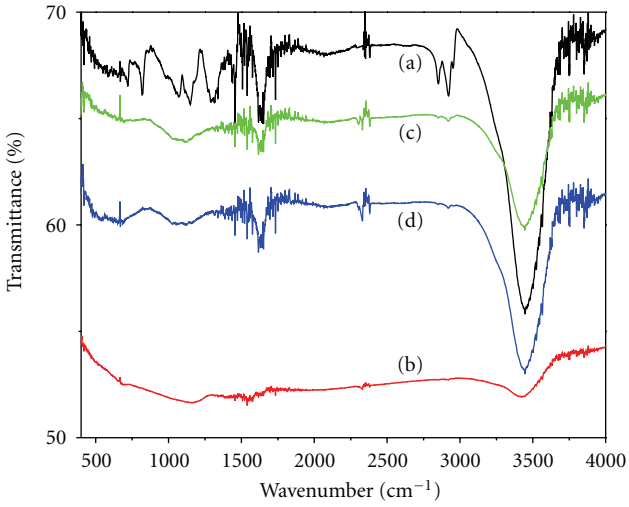

FIGURE 5: FT-IR spectra of (a) bulk P3HT and P3HT-MWNT composites of (b) P3HT-rMWNT, (c) P3HT-siMWNT, and (d) P3HT-fMWNT.

space-group symmetry [29] and the peak around 1562–1590 cm^{-1} is assigned with C=C stretch [30, 31]. It is found at 1621 cm^{-1} in the as-procured MWNT sample as received (not shown here). The further figures correspond to P3HT and its composites. In the case of P3HT the absorption bands 2920 and 2849 cm^{-1} correspond to –CH_2-stretch vibration and shoulder at 2956 cm^{-1} corresponds with the –CH_3 asymmetry stretch vibration. The bands centered at 1453 and 1320 cm^{-1} can be attributed to the bending vibration mode of –CH_2- and –CH_3. The characteristic in-plane and out-of-plane rocking vibration of –$(CH_2)_n$-group ($n \geq 4$) can also be observed at 717 and 1148 cm^{-1} in this spectra. For P3HT there is no observation of the split of 717 cm^{-1} band into 720 and 730 cm^{-1}, which are representative of the ordered and disordered —CH_2-groups rocking vibration band [32]. According to Furukawa et al. [33] and Trznadel et al. [34] the ratio between the intensity of the antisymmetric C=C stretching peak (mode at 1510 cm^{-1}) and the intensity of the symmetric stretching peak (mode at 1456 cm^{-1}) can be used to probe the average conjugation length of P3HT. The same type of observation has been reported by Musumeci et al. in their work of P3HT/MWNT composites [35]. In this case there is no change in the ν_{sym}(C=C) and $\nu_{antisym}$(C=C) frequencies of the P3HT with successive loading of carbon nanotubes suggesting that there is no significant ground state interaction between the polymer and the CNT. The intensity ratio of I$\nu_{antisymm}$(C=C)/Iν_{sym}(C=C) versus wt% of MWNT is generally found a slight increment per unit addition of carbon nanotubes and the 1456 cm^{-1} and 1510 cm^{-1} corresponding to stretch vibration of the thiophene ring are notified as tangible shift [36]. Hence it is not possible to think of any strong interaction between the carbon nanotube and the polymer, for some weak π-π ground state interaction between the moieties.

As Raman spectroscopy is sensitive to both electronic and vibrational structures of carbon nanotubes, it can be conveniently used to probe the structure of polymer-nanocomposites. The spectra of P3HT and the polymer composites are shown in Figure 6. In the signals of P3HT-rMWNT composites the important peaks at 1350 and 1582 cm^{-1} represent the sp^3 mode (D band) and the tangential mode (G band) of the nanotubes, respectively [37]. The intensity ratio of the D over G band (D/G ratio) has been used to predict the extent of purity of the nanotubes as well. With P3HT-fMWNT and P3HT-siMWNT composites the shift of G and D band frequencies is seen as a direct consequence of interaction between carbon tubes and the polymer. musumeci et al. have reported the effect as of an electron donor-acceptor type [35]. Specifically, the charge removal from MWNT results in an upshift in the G band and a downshift in the Raman D band which is attributed to additional electron density in the MWNT antibonding orbitals from charge injection [38]. In the present study, the frequency of the G band has shown a tangible shift and is centered on 1582 cm^{-1} suggesting that the polymer has entered into might charge transfer with the nanotubes.

The UV-Vis absorption spectra of P3HT and P3HT/MWNT composites in 1,2,4-trichlorobenzene are presented in Figure 7. It is known that MWNT absorption makes no significant contributions to the spectra [39]. The value of λ_{max} of P3HT (456 nm) is in line with an already reported value in the literature [40, 41]. There is a significant shift in the λ_{max} of the polymer upon inclusion of carbon nanotubes in the form of composites. This suggests boasting of ground state interaction and hence appreciable charge transfer between the polymer and the MWNT.

The PL spectra of P3HT and its composites in 1,2,4-trichlorobenzene ($C_6H_3Cl_3$) for an excitation wavelength of 450 nm are presented in Figure 8. The polymer and the composites P3HT-rMWNT, P3HT-fMWNT, and P3HT-siMWNT show emissions in the range 527–575 nm. The reason for the photoluminescence quenching of the composites may be attributed to π-π interactions of P3HT with the nanotubes forming additional decaying paths of

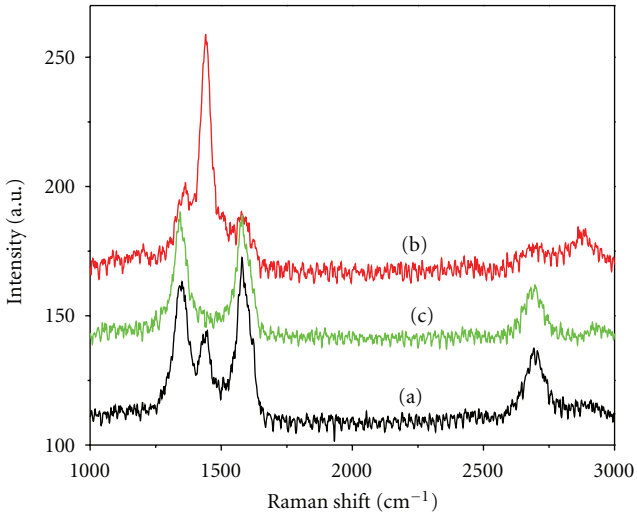

Figure 6: Raman data of (a) P3HT-rMWNT, (b) P3HT-siMWNT, and (c) P3HT-fMWNT composites.

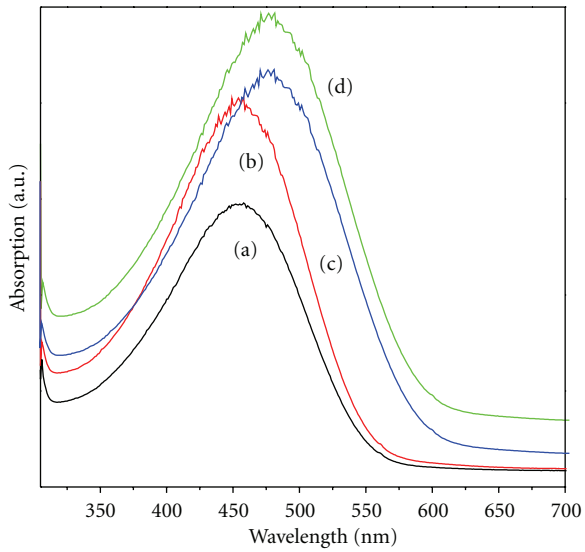

Figure 7: UV-vis absorption data of (a) bulk P3HT and P3HT-MWNT composites of (b) P3HT-rMWNT, (c) P3HT-fMWNT, and (d) P3HT-siMWNT.

the excited electrons through the MWNT, the silanized MWNT is the effective photoluminescence quenching [42]. This larger quenching indicates that the singlet exitons generated in the polymer are diminished before radiative recombination due to the presence of MWNT in addition to absorption and scattering by the nanotubes. Furthermore in this case, the MWNT acts as a nanometric heat sink which dissipates the heat generated from the incident beam [43]. The absence of any significant shift of the maximal luminescence peaks for the composites at different excitation wavelengths suggests extended molecular packing between the polymer and MWNT to be of a physical nature and

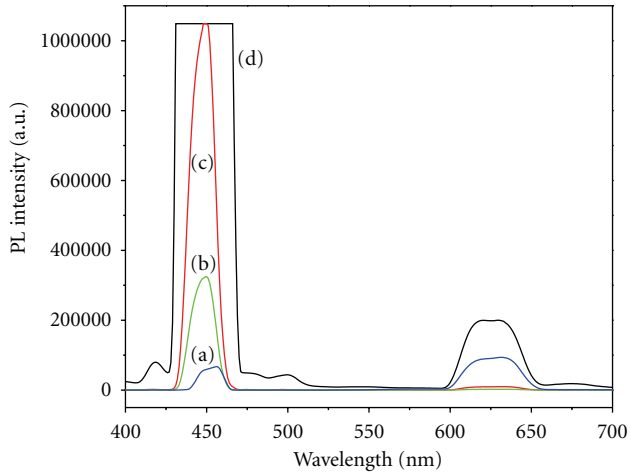

Figure 8: Photoluminescence spectra of (a) bulk P3HT and P3HT-MWNT composites of (b) P3HT-rMWNT, (c) P3HT-fMWNT, and (d) P3HT-siMWNT.

Table 1: Room temperature conductivity of P3HT and P3HT-MWNT composites.

Samples	P3HT	P3HT-rMWNT	P3HT-fMWNT	P3HT-siMWNT
Conductivity (S/cm)	2.3×10^{-5}	0.37	0.12	0.71

the absence of any important configurational relaxation in the excited state [44].

The electrical conductivity of conducting polymers depends on the extent of conjugation and the amount of dopant present in them [45]. Further in the case of polymer/CNT composites, it depends on the purity of the nanotubes and their alignments [46]. The DC electrical conductivity results of P3HT and its composites are presented in Table 1. The conductivity of the polymer and its composites are measured using approximately 0.04 g of the samples, pressed into pellet form of 1.2 cm in diameter and 0.556 mm thickness using 600 kgf/cm^2 pressure by a manual hydraulic press for 15 min. The conductivity of P3HT at room temperature (25°C) is noted to be 2.3×10^{-5} S/cm. The conductivity of the polymer is increased with successive acid-treated functionalized and silane modified of the MWNT, reaches a maximum value of 0.12 and 0.71 S/cm, respectively and a five fold increase. Some of the individual MWNT or nanotube clusters isolated by polymer coatings are responsible for hoping transfer of electrons besides their tunneling through the nanotubes for a three-dimensional percolation system [47].

P3HT-MWNT in-situ polymerized composites exhibit good dispersibility in CHCl3, THF, and chlorobenzene and so forth solvents much better than the simple blend of the polymer and MWNT prepared through the sonication process. The hydrophobisity of the nanotubes much reduced through the good wrapping of the polymer on the walls of the nanotube leading to a long stability of the solution and a much better dispersibility also. The functionalized and

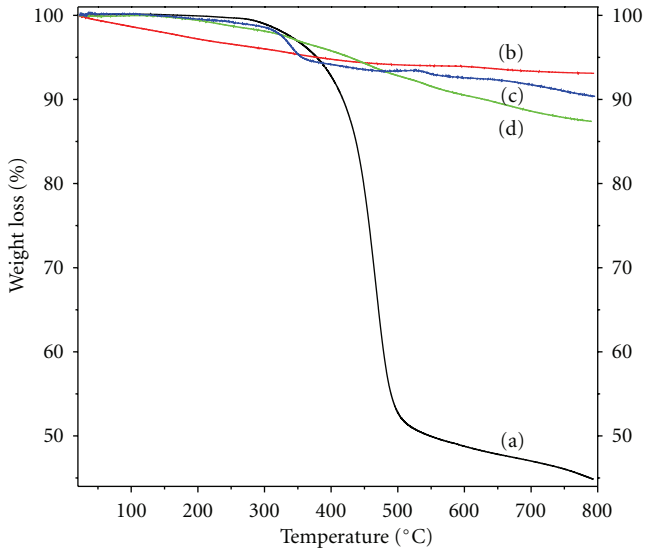

Figure 9: TGA analysis data of (a) bulk P3HT and P3HT-MWNT composites of (b) P3HT-rMWNT, (c) P3HT-fMWNT, and (d) P3HT-siMWNT.

silanized composites have exhibited stability over 10 weeks, while the blend was stable for not more than 7 days. This will really be an advantage while casting solar active coatings over a larger area substrate on a scaled-up level in field trials.

The TGA results of P3HT and the composites are presented in Figure 9. The results indicate the presence of MWNT in the polymer matrix for the composites to cause enhanced thermal stability. Such increase in thermal stability has already been reported with few polymer CNT composites [13, 15, 17, 20]. The higher residual weight in the case of the composites is due to the presence of underrated nanotubes and metallic impurities present in the as-procured MWNT.

4. Conclusions

Conducting polymer-modified carbon nanotubes (P3HT-MWNT) composites have been synthesized through in situ polymerization procedure using $FeCl_3$ oxidant for photovoltaic cells applications. The lack of any significant ground state interaction involving any charge transfer, but only π-π stacking of noncovalent interaction type between the polymer and the walls of the nanotube, is evident from FT-IR, Raman, UV-Vis, PL spectra, and other measurements. The in-situ polymerization procedure of the donor polymer molecules and the acceptor carbon nanotubes has resulted in enhanced dispersibility and stability of the composites in organic solvents compared to the simple sonication of them providing convenient and reliable approach for their use in solar cell applications.

Acknowledgment

The authors gratefully acknowledge the financial support from NPST program by King Saud University of project no. 10-NAN1021-02.

References

[1] G. Yu, J. Gao, J. C. Hummelen, F. Wudl, and A. J. Heeger, "Polymer photovoltaic cells: enhanced efficiencies via a network of internal donor-acceptor heterojunctions," *Science*, vol. 270, no. 5243, pp. 1789–1791, 1995.

[2] L. M. Campos, A. Tontcheva, S. Günes et al., "Extended photocurrent spectrum of a low band gap polymer in a bulk heterojunction solar cell," *Chemistry of Materials*, vol. 17, no. 16, pp. 4031–4033, 2005.

[3] W. U. Huynh, J. J. Dittmer, and A. P. Alivisatos, "Hybrid nanorod-polymer solar cells," *Science*, vol. 295, no. 5564, pp. 2425–2427, 2002.

[4] J. Liu, T. Tanaka, K. Sivula, A. P. Alivisatos, and J. M. J. Fréchet, "Employing end-functional polythiophene to control the morphology of nanocrystal—polymer composites in hybrid solar cells," *Journal of the American Chemical Society*, vol. 126, no. 21, pp. 6550–6551, 2004.

[5] E. Kymakis and G. A. J. Amaratunga, "Single-wall carbon nanotube/conjugated polymer photovoltaic devices," *Applied Physics Letters*, vol. 80, no. 1, pp. 112–114, 2002.

[6] E. Kymakis, I. Alexandrou, and G. A. J. Amaratunga, "High open-circuit voltage photovoltaic devices from carbon-nanotube-polymer composites," *Journal of Applied Physics*, vol. 93, no. 3, pp. 1764–1768, 2003.

[7] B. J. Landi, R. P. Raffaelle, S. L. Castro, and S. G. Bailey, "Single-wall carbon nanotube-polymer solar cells," *Progress in Photovoltaics*, vol. 13, no. 2, pp. 165–172, 2005.

[8] B. J. Landia, S. L. Castrob, H. J. Rufa, C. M. Evansa, S. G. Baileyc, and R. P. Raffaelle, "CdSe quantum dot-single wall carbon nanotube complexes for polymeric solar cells," *Solar Energy Materials and Solar Cells*, vol. 87, p. 733, 2005.

[9] M. M. Alam and S. A. Jenekhe, "Efficient solar cells from layered nanostructures of donor and acceptor conjugated polymers," *Chemistry of Materials*, vol. 16, no. 23, pp. 4647–4656, 2004.

[10] T. Kietzke, H.-H. Hörhold, and D. Neher, "Efficient polymer solar cells based on M3EH-PPV," *Chemistry of Materials*, vol. 17, no. 26, pp. 6532–6537, 2005.

[11] A. G. Manoj, A. A. Alagiriswamy, and K. S. Narayan, "Photogenerated charge carrier transport in p-polymer n-polymer bilayer structures," *Journal of Applied Physics*, vol. 94, no. 6, pp. 4088–4095, 2003.

[12] J. Geng and T. Zeng, "Influence of single-walled carbon nanotubes induced crystallinity enhancement and morphology change on polymer photovoltaic devices," *Journal of the American Chemical Society*, vol. 128, no. 51, pp. 16827–16833, 2006.

[13] M. R. Karim, C. J. Lee, Y.-T. Park, and M. S. Lee, "SWNTs coated by conducting polyaniline: synthesis and modified properties," *Synthetic Metals*, vol. 151, no. 2, pp. 131–135, 2005.

[14] M. S. P. Shaffer and K. Koziol, "Polystyrene grafted multi-walled carbon nanotubes," *Chemical Communications*, no. 18, pp. 2074–2075, 2002.

[15] M. R. Karim, J. H. Yeum, M. S. Lee, and K. T. Lim, "Synthesis of conducting polythiophene composites with multi-walled carbon nanotube by the γ-radiolysis polymerization method," *Materials Chemistry and Physics*, vol. 112, no. 3, pp. 779–782, 2008.

[16] I. C. Liu, H. M. Huang, C. Y. Chang, H. C. Tsai, C. H. Hsu, and R. C. C. Tsiang, "Preparing a styrenic polymer composite containing well-dispersed carbon nanotubes: anionic polymerization of a nanotube-bound p-methylstyrene," *Macromolecules*, vol. 37, no. 2, pp. 283–287, 2004.

[17] M. R. Karim, C. J. Lee, A. M. S. Chowdhury, N. Nahar, and M. S. Lee, "Radiolytic synthesis of conducting polypyrrole/carbon nanotube composites," *Materials Letters*, vol. 61, no. 8-9, pp. 1688–1692, 2007.

[18] H. Kong, C. Gao, and D. Yan, "Controlled functionalization of multiwalled carbon nanotubes by in situ atom transfer radical polymerization," *Journal of the American Chemical Society*, vol. 126, no. 2, pp. 412–413, 2004.

[19] B. Zhao, H. Hu, and R. C. Haddon, "Synthesis and properties of a water-soluble single-walled carbon nanotube-poly(m-aminobenzene sulfonic acid) graft copolymer," *Advanced Functional Materials*, vol. 14, no. 1, pp. 71–76, 2004.

[20] M. R. Karim, C. J. Lee, and M. S. Lee, "Synthesis and characterization of conducting polythiophene/carbon nanotubes composites," *Journal of Polymer Science A*, vol. 44, no. 18, pp. 5283–5290, 2006.

[21] A. Bolognesi, W. Porzio, A. Provasoli et al., "Structural and thermal behavior of poly-(3-octylthiophene): a DSC, ^{13}C MAS NMR, XRD, photoluminescence, and Raman scattering study," *Macromolecular Chemistry and Physics*, vol. 202, no. 12, pp. 2586–2591, 2001.

[22] S. A. Chen and J. M. Ni, "Structure/properties of conjugated conductive polymers. 1. Neutral poly(3-alkylthiophene)s," *Macromolecules*, vol. 25, no. 23, pp. 6081–6089, 1992.

[23] T. Shiga and A. Okada, "Electroplastic behavior of doped poly(3-hexylthiophene)," *Journal of Applied Polymer Science*, vol. 62, no. 6, pp. 903–910, 1996.

[24] K. Tashiro, K. Ono, Y. Minagawa, M. Kobayashi, T. Kawai, and K. Yoshino, "Structure and thermochromic solid-state phase transition of poly(3-alkylthiophene)," *Journal of Polymer Science B*, vol. 29, no. 10, pp. 1223–1233, 1991.

[25] J. Mårdalen, E. J. Samuelsen, O. R. Gautun, and P. H. Carlsen, "Chain configuration of poly(3-hexylthiophene) as revealed by detailed X-ray diffraction studies," *Solid State Communications*, vol. 77, no. 5, pp. 337–339, 1991.

[26] W. P. Hsu, K. Levon, K. S. Ho, A. S. Myerson, and T. K. Kwei, "Side-chain order in poly(3-alkylthiophenes)," *Macromolecules*, vol. 26, no. 6, pp. 1318–1323, 1993.

[27] R. Andrews, D. Jacques, D. Qian, and E. C. Dickey, "Purification and structural annealing of multiwalled carbon nanotubes at graphitization temperatures," *Carbon*, vol. 39, no. 11, pp. 1681–1687, 2001.

[28] Y. Huang, N. Li, Y. Ma et al., "The influence of single-walled carbon nanotube structure on the electromagnetic interference shielding efficiency of its epoxy composites," *Carbon*, vol. 45, no. 8, pp. 1614–1621, 2007.

[29] J. Zhang, H. Zou, Q. Qing et al., "Effect of chemical oxidation on the structure of single-walled carbon nanotubes," *Journal of Physical Chemistry B*, vol. 107, no. 16, pp. 3712–3718, 2003.

[30] X. Li, J. Zhang, Q. Li, H. Li, and Z. Liu, "Polymerization of short single-walled carbon nanotubes into large strands," *Carbon*, vol. 41, p. 598, 2003.

[31] X. Yu, R. Rajamani, K. A. Stelson, and T. Cui, "Fabrication of carbon nanotube based transparent conductive thin films using layer-by-layer technology," *Surface and Coatings Technology*, vol. 202, no. 10, pp. 2002–2007, 2008.

[32] X. Qiao, X. Wang, and Z. Mo, "Effects of different alkyl substitution on the structures and properties of poly(3-alkylthiophenes)," *Synthetic Metals*, vol. 118, no. 1–3, pp. 89–95, 2001.

[33] Y. Furukawa, M. Akimoto, and I. Harada, "Vibrational key bands and electrical conductivity of polythiophene," *Synthetic Metals*, vol. 18, no. 1–3, pp. 151–156, 1987.

[34] M. Trznadel, A. Pron, M. Zagorska, R. Chrzaszcz, and J. Pielichowski, "Effect of molecular weight on spectroscopic and spectroelectrochemical properties of regioregular poly(3-hexylthiophene)," *Macromolecules*, vol. 31, no. 15, pp. 5051–5058, 1998.

[35] A. W. Musumeci, G. G. Silva, J. W. Liu, W. N. Martens, and E. R. Waclawik, "Structure and conductivity of multi-walled carbon nanotube/poly(3-hexylthiophene) composite films," *Polymer*, vol. 48, no. 6, pp. 1667–1678, 2007.

[36] B. K. Kuila, S. Malik, S. K. Batabyal, and A. K. Nandi, "In-situ synthesis of soluble poly(3-hexylthiophene)/multiwalled carbon nanotube composite: morphology, structure, and conductivity," *Macromolecules*, vol. 40, no. 2, pp. 278–287, 2007.

[37] Y. L. Liu and W. H. Chen, "Modification of multiwall carbon nanotubes with initiators and macroinitiators of atom transfer radical polymerization," *Macromolecules*, vol. 40, no. 25, pp. 8881–8886, 2007.

[38] K. E. Wise, C. Park, E. J. Siochi, and J. S. Harrison, "Stable dispersion of single wall carbon nanotubes in polyimide: the role of noncovalent interactions," *Chemical Physics Letters*, vol. 391, no. 4–6, pp. 207–211, 2004.

[39] E. V. Ovsyannikova, O. N. Efimov, A. P. Moravsky, R. O. Loutfy, E. P. Krinichnaya, and N. M. Alpatova, "Electrochemical properties of thin-layered composites formed by carbon nanotubes and polybithiophene," *Russian Journal of Electrochemistry*, vol. 41, no. 4, pp. 439–446, 2005.

[40] A. Babel and S. A. Jenekhe, "Alkyl chain length dependence of the field-effect carrier mobility in regioregular poly(3-alkylthiophene)s," *Synthetic Metals*, vol. 148, no. 2, pp. 169–173, 2005.

[41] E. Kymakis and G. A. J. Amaratunga, "Optical properties of polymer-nanotube composites," *Synthetic Metals*, vol. 142, no. 1–3, pp. 161–167, 2004.

[42] J. Chen, H. Liu, W. A. Weimer, M. D. Halls, D. H. Waldeck, and G. C. Walker, "Noncovalent engineering of carbon nanotube surfaces by rigid, functional conjugated polymers," *Journal of the American Chemical Society*, vol. 124, no. 31, pp. 9034–9035, 2002.

[43] W. Feng, A. Fujii, M. Ozaki, and K. Yoshino, "Perylene derivative sensitized multi-walled carbon nanotube thin film," *Carbon*, vol. 43, no. 12, pp. 2501–2507, 2005.

[44] K. Colladet, S. Fourier, T. J. Cleij et al., "Low band gap donor-acceptor conjugated polymers toward organic solar cells applications," *Macromolecules*, vol. 40, no. 1, pp. 65–72, 2007.

[45] F. Mohammad, P. D. Calvert, and N. C. Billingham, "Electrical and electronic properties of polyparaphenylenes," *Journal of Physics D*, vol. 29, no. 1, pp. 195–204, 1996.

[46] H. Peng, "Aligned carbon nanotube/polymer composite films with robust flexibility, high transparency, and excellent conductivity," *Journal of the American Chemical Society*, vol. 130, no. 1, pp. 42–43, 2008.

[47] S. Barrau, P. Demont, A. Peigney, C. Laurent, and C. Lacabanne, "Dc and ac conductivity of carbon nanotubes-polyepoxy composites," *Macromolecules*, vol. 36, no. 14, pp. 5187–5194, 2003.